Scientific Contributions Oil & Gas, Vol. 48. No. 4, December: 229 - 250

SCIENTIFIC CONTRIBUTIONS OIL AND GAS

Testing Center for Oil and Gas
LEMIGAS

Journal Homepage:http://www.journal.lemigas.esdm.go.id
ISSN: 2089-3361, e-ISSN: 2541-0520

Comparative Analysis of The Use of Nanosilica and Potassium Chloride as Shale Inhibitor in Water Based Mud

Nur Suhascaryo[1], Syifa Khasyikirana Ramadhanti[1], Ketut Rama Wijaya[2] and Miftahul Jannah[2]

[1]Petroleum Engineering, Faculty of Mineral and Energy Technology, UPN "Veteran" Yogyakarta
Padjajaran 104 Street, Condongcatur, Sleman, Yogyakarta 55283, Indonesia.

[2]PT. Pertamina (Persero)
Medan Merdeka Tim. Street Gambir District, Central Jakarta City, 10110, Indonesia.

Corresponding Author: KRT Nur Suhascaryo (nur.suhascaryo@upnyk.ac.id)

Manuscript received: October 16th, 2025; Revised: November 07th, 2025
Approved: December 05th, 2025; Available online: December 15th, 2025; Published: December 16th, 2025.

ABSTRACT - Swelling shale is one of the most common problems encountered in oil and gas drilling operations. Potassium chloride (KCl) is widely applied as a shale inhibitor due to its ionic inhibition mechanism; however, excessive KCl concentrations can have detrimental effects on drilling mud performance. This study examines the potential of nanosilica derived from geothermal industrial waste as a substitute for KCl. Five mud samples were tested: base fluid, 1% nanosilica, 3% nanosilica, 1% KCl, and 3% KCl. The samples were evaluated through a series of physical property tests, including density, rheology, filtration loss, pH, methylene blue test (MBT), K^+ concentration, and Cl^- concentration. Swelling-related parameters were also assessed using Linear Swelling Meter (LSM), accretion tests, and erosion tests under both before hot rolling (BHR) and after hot rolling (AHR) conditions at 200°F for 16 hours. The results indicate that nanosilica improved rheological properties and reduced shale swelling compared to the base fluid. Meanwhile, the 1% KCl formulation demonstrated strong performance in LSM and erosion tests. Overall, nanosilica shows potential as a partial substitute for KCl as a shale inhibitor; however, surface modification and field-scale validation are recommended for further confirmation.

Keywords: nanosilica, potassium chloride, shale inhibitor, swelling shale, water based mud.

How to cite this article:

Nur Suhascaryo, Syifa Khasyikirana Ramadhanti, Ketut Rama Wijaya and Miftahul Jannah, 2025, Comparative Analysis of The Use of Nanosilica and Potassium Chloride as Shale Inhibitor in Water Based Mud, Scientific Contributions Oil and Gas, 48 (4) pp. 229-250. https://doi.org/10.29017/scog.v48i4.1768.

INTRODUCTION

Drilling mud is a critical component in oil and gas drilling operations, consisting of a mixture of water, clay, and various chemical additives. Its primary functions include maintaining wellbore stability, transporting cuttings to the surface, cooling and lubricating drilling equipment, controlling bottom-hole pressure, minimizing formation damage, preventing corrosion, and reducing environmental impacts (Hughes 2006). The performance and stability of drilling operations strongly depend on the proper formulation of water -based mud (WBM), particularly in terms of mud weight, rheology, and filtration properties, which must be adjusted according to formation pressure and lithological variations. Studies on high-performance WBM have shown that maintaining mud weight within a safe operational window is essential to prevent well control issues such as kicks and lost circulation, with weighting agents such as barite playing a key role in ensuring wellbore stability (Wahyuni et al., 2025).Shale inhibitor in drilling used when drilling through shale formations. Shale is a type of detrital sedimentary rock formed the consolidation of fine materials, including clay, mud, and silt. Shale is known porous yet non-permeable characteristics. Shale formations are understood about 99% clay minerals and only 1% organic matter (Halliburton, 2011). The clay minerals most commonly found within shale include smectite (montmorillonite), illite, kaolinite, and chlorite. Clay is defined as a mineral composed of inorganic substances, excluding peat, muck, or soil that contains high levels of organic or naturally occurring minerals (Kumari & C.M., n.d.). Clay has a soft texture with fine grains and is less than 0.005 mm in diameter and has a particle size of <2μm (MI Swaco 1998). The type of clay present in a mineral or shale can be identified through its CEC (Cation Exchange Capacity) value. The classification of clay minerals can be seen in Table 1.

Clay has a stacked or layered structure, with each layer having a thickness of approximately ±10 angstroms (Å). These layers are described an extremely thin and flexible form, possessing a large surface area and functioning the ability to absorb water. When water is absorbed, the clay begins swelling until it reaches the weakest point of its structural reinforcement, which eventually causes the individual clay layers to separate from the larger group (MI Swaco 1998). Clay is known two types of structural layers. The first is the two-layer type (kaolinite), where each layer consists a combination of a tetrahedral silica layer (pyramidal structure) and an octahedral alumina or magnesium layer (eight-faced structure. The second is the three -layer type (montmorillonite, chlorite, illite), in which each layer consists two tetrahedral layers and one octahedral layer stacked on top of one another. In contrast, the two-layer type contains only one tetrahedral layer and one octahedral layer (MI Swaco 1998).

Smectite (montmorillonite) is recognized the highest reactivity to water among all clay types. Smectite, which belongs an expandable clay mineral group, can absorb water and expand up to ten times its original volume (Hughes 2006). The swelling of shale can be reduced by selecting the proper type and quantity of cations. Cations with the highest capability in controlling swelling include lithium, sodium, potassium, magnesium, calcium, aluminum, and hydrogen. Therefore, an appropriate mud composition is required to

Table 1. General classification of shale (Mondshine 1966)

Formation type	**CEC (Meq/100 gr)**	**Clay type**
Soft	20 – 40	Montmorillonite & illite
Firm	15 – 20	Illite & mixed layer montmorillonite illite
Hard	3 – 10	Trace montmorillonite, high illite
Brittle	0 – 3	Illite, kaoline, chlorite
Firm hard	10 – 20	Illite & mixed layer montmorillonite illite

manage shale swelling, one of which is to use a suitable shale inhibitor. Potassium chloride (KCl) is one of the most widely used shale inhibitors. It has a particle size ranging from 50–75 nm, with maximum dispersion observed at approximately 130 nm (Jakubiak et al., 2016). KCl is commonly applied in drilling mud systems due to its good compatibility with formation water and chemical stability. Compatibility tests showed no precipitation (0.0000 g/L) at formation water contents up to 25%, with only a slight increase to 0.0100 g/L at higher concentrations, indicating that KCl remains chemically stable and suitable for water-based mud applications (Wahyudi & Makmur, 2004). Experimental results by Kartini (2014) demonstrated that shale containing 15% smectite (sample KG-1C) experienced a reduction in swelling from 10.6% in distilled water to 6.2% when treated with KCl–polymer mud, and further to 3.2% when treated with brine mud. Linear Swelling Meter (LSM) and XRD analyses confirmed that KCl ions replaced Ca^{2+} and Na^{+} within the smectite structure, eliminating smectite peaks and reducing carbonate minerals such as calcite. These results indicate that KCl–polymer mud can reduce shale swelling by more than 90%. Similar findings were reported by Wahyuni et al. (2025), who showed that KCl-based high-performance water-based mud (HPWBM) effectively minimized swelling and improved wellbore stability in reactive shale formations. The inhibition mechanism of KCl involves the dissociation of KCl in the aqueous phase into K^{+} and Cl^{-} ions. K^{+} ions are preferentially adsorbed onto clay interlayers through cation exchange, replacing Na^{+} and Ca^{2+}, reducing diffuse double-layer thickness and interlayer bound water. This process decreases clay hydration and swelling tendency. Due to its relatively large ionic diameter, K^{+} can penetrate clay interlayers and microfractures, limiting water ingress and enhancing shale stability. The cation exchange selectivity follows the order $H^{+} > Al^{3+} > Ca^{2+} > Mg^{2+} > K^{+} > NH_4^{+} > Na^{+} > Li^{+}$, where cations on the left replace those on the right (MI Swaco 1998).

Table 2. Ionic diameter and hydrated diameter of cations (MI Swaco 1998)

Cation	Ionic diameter (Å)	Hydrated diameter (Å)
Li+	1,56	14,6
Na+	1,90	11,2
K+	2,66	7,6
NH4+	2,86	5,0
Mg2+	1,30	21,6
Ca2+	1,98	19,2
Al3+	1,00	18,0

In line with technological progress, research on nanosilica as a shale inhibitor continues to be developed . The nanosilica (SiO_2) used in this study is produced from geothermal industrial silica waste, which undergoes several processing steps to reach nanoscale size (<100 nm) with a particle size distribution ranging from 32–78 nm, as illustrated in Figure 2. This nanosilica possesses a purity level of up to 99%, with a chemical composition consisting of SiO_2 (99.18%), K_2O (0.15%), MnO (0.036%), Fe_2O_3 (0.15%), CuO (0.08%), and CaO (0.406%).

During the hydrolysis stage, NaOH was used to form a sodium silicate (Na_2SiO_3) sol (Mujiyanti, 2010). According to Trivana et al. (2015), SiO_2 as an alkoxide precursor is dissolved in NaOH which aims to help in the formation of sodium silicate

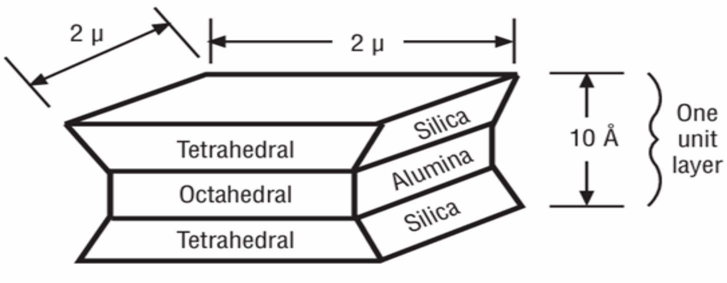

Figure 1. Three-layer type illustration (MI Swaco 1998)

soles, where the reaction resulting from the dissolution is $SiO_2 + 2\ NaOH \rightarrow Na_2SiO_3 + H_2O$. Meanwhile the condensation stage is the transition stage from the sole process to gel. HCl was used to stimulate the formation of silicic acid monomers, which subsequently lead to gel formation. According to Prastiyanto (2008), the gel formation reaction at this stage results in: $Na_2SiO_3 + HCl + H_2O \rightarrow Si(OH)_4 + HCl$. Finally, the aging and drying stage aims to remove residual solutions and liquids produced during the sol–gel process. This step was carried out using an evaporation method. Nanosilica as shale inhibitor works through two mechanisms, physically and chemically.

Physically, nanosilica is able to work by plugging pore cavities in shale and creating structural bridges because its particle size is smaller than one-third of the shale pore diameter (Nader, 2012). Chemically, by forming a new hydroxyl (-OH) layer on the nanosilica surface (Guo et al., 2018), this hydroxyl group can be generated either during the sol–gel process or when it reacts with additives after being mixed into the drilling mud. The incorporation of nanopowders, particularly nano-silica at a concentration of 0.2 wt% in brine, has been shown to enhance heating rate and increase the imbibition recovery factor from 14.2% to 33.74% under 900 W electromagnetic heating for 55 seconds, indicating its ability to modify fluid–rock interactions and fluid rheology in aqueous systems (Nirmala et al., 2025). Nanosilica has also been reported to improve rheological stability, prevent sudden rheological degradation, and reduce filtrate volume at elevated temperatures (Taragikhah et al., 2017). Increasing nanosilica concentration results in higher plastic viscosity and yield point, reduced filtration loss, and improved cutting-lifting capacity (Affez et al., 2018). Under after hot rolling (AHR) conditions, the addition of nanosilica reduced filtration loss by 17.6% and 15% and decreased filter cake thickness by 48.5% and 45.4%, while enhancing rheological parameters, including yield point (23.3%), gel strength at 10 s (21%), and gel strength at 10 min (36%) (Prakash et al., 2021). Furthermore, drilling mud containing nanosilica

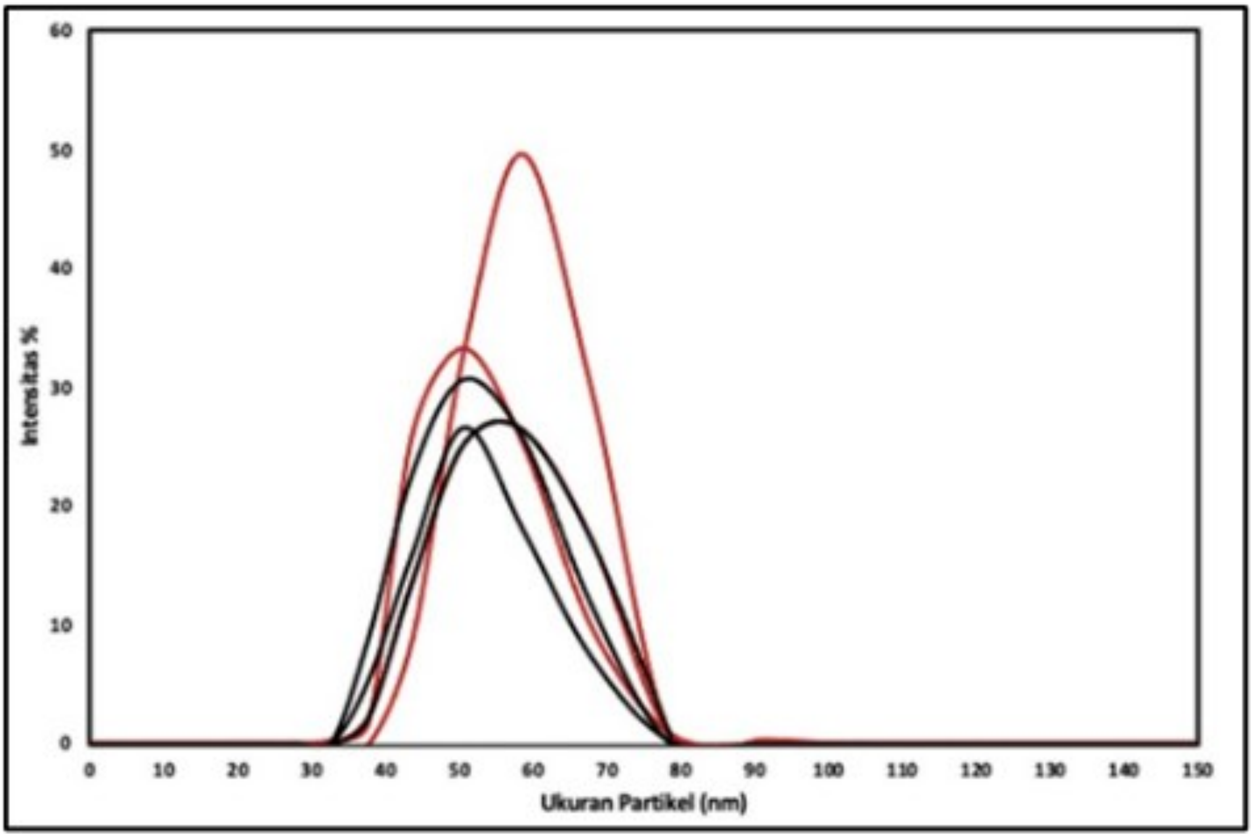

Figure 2. Nanosilica particle size distribution (PT Pertamina (Persero) 2025)

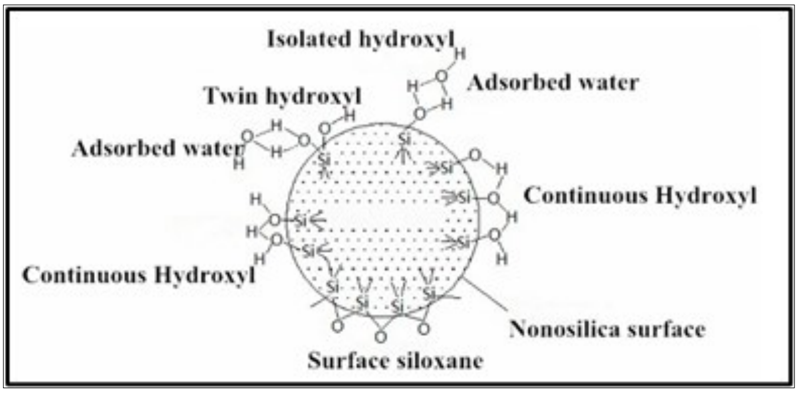

Figure 3. Nanosilica chemically working mechanism (Guo et al., 2018)

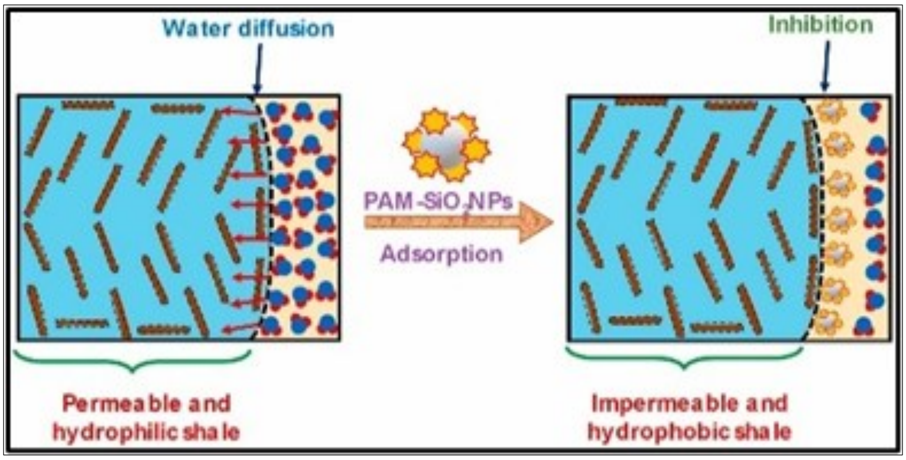

Figure 4. Nanosilica physically working mechanism (Saleh 2022)

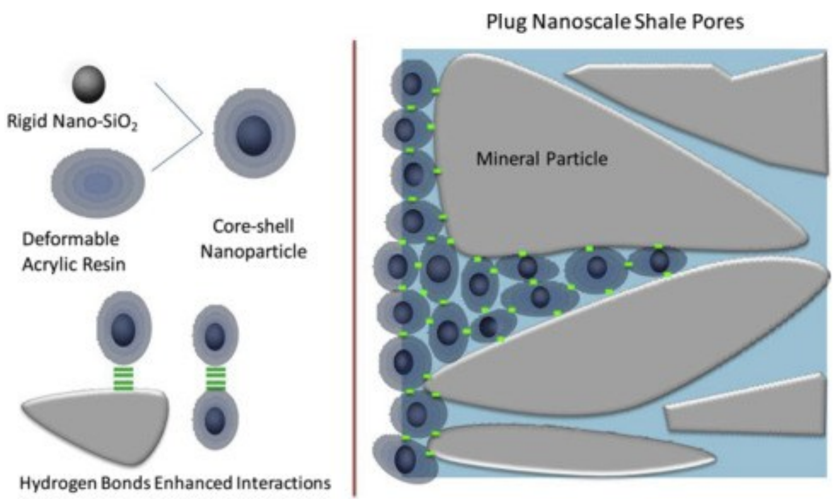

Figure 5. Clay mineral and nanosilica interaction (Zhang & Li 2024)

achieved the highest shale-dispersion recovery value (86.6%), compared to 27.1%, 49.2%, 73.5%, and 74.7% for water and KCl-based mud systems, and reduced bentonite swelling by 55% relative to water-based tests (Saleh et al., 2021). Accordingly, this study aims to evaluate the influence of nanosilica on drilling mud physical properties, compare the performance of nanosilica and KCl-containing mud systems through physical and swelling-related tests, and assess the potential of nanosilica as a substitute for KCl as a shale inhibitor in water-based mud systems.

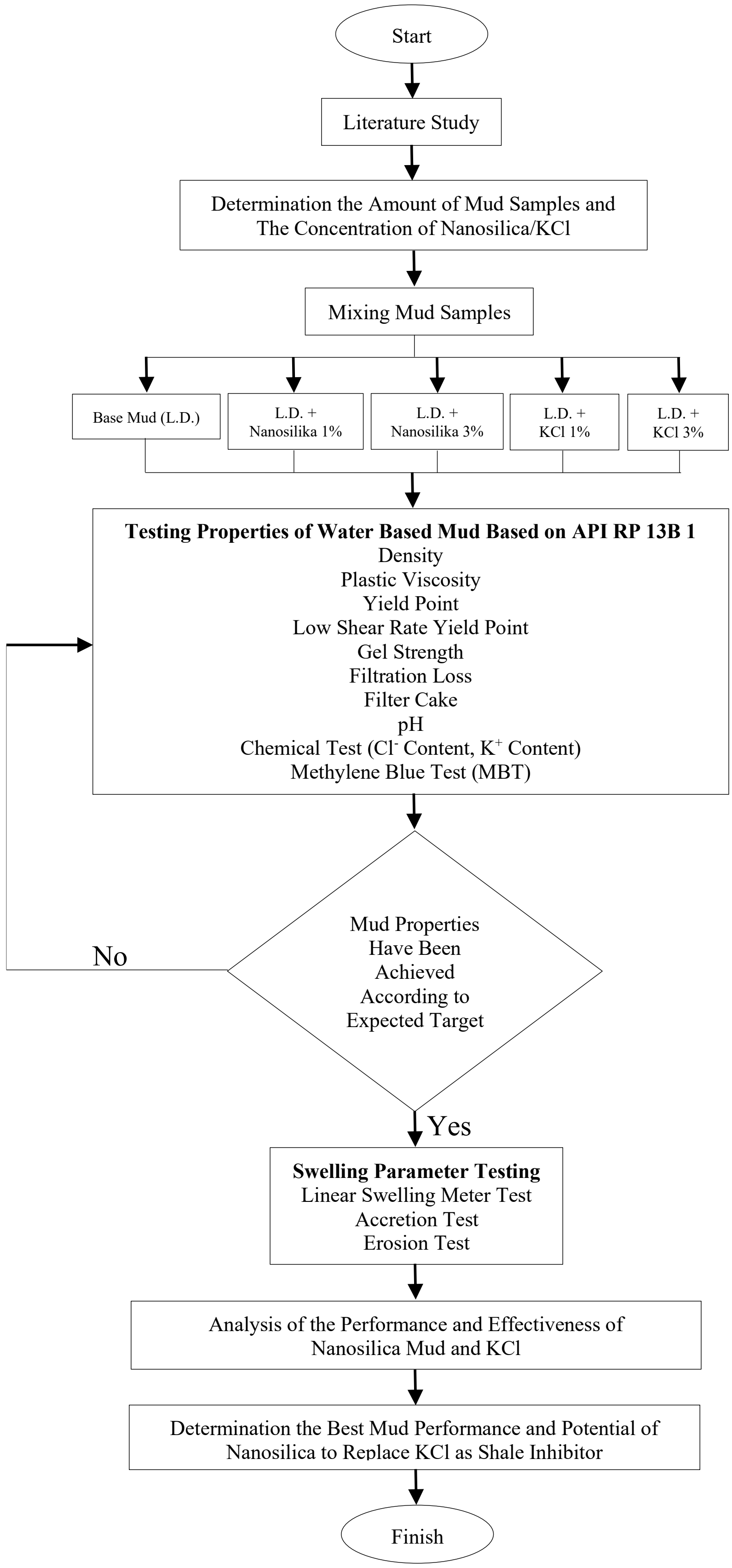

Figure 6. Workflow used in this study.

METHODOLOGY

This research is designed to a laboratory experimental study. In this work, five drilling mud samples were utilized, and all five were evaluated for their performance through physical property testing, which includes density measurement, rheology, filtration loss and filter cake analysis, pH assessment, methylene blue test (MBT), potassium (K^+) content, and chloride (Cl^-) ion content. Swelling-related parameters were also examined, consisting of linear swelling meter testing, accretion testing, and erosion testing. All five samples were tested in both before hot rolled (BHR) and after hot rolled (AHR) conditions, with oven treatment conducted at 200°F for 16 hours.

The methodology begins with a literature review to understand the characteristics, particle size, processing methods, and mechanisms of nanosilica. This step is followed by determining the number of drilling mud samples and the concentrations of nanosilica and KCl used in each formulation. The process then continues with the mixing and testing of water-based mud properties, which include measurements of density, rheology (plastic viscosity, yield point, low shear rate yield point, gel strength), filtration loss, filter cake, pH, as well as chemical analyses consisting of chloride ion content, potassium content, and the methylene blue test. All property tests were conducted based on API RP 13B-1 standards. Once the mud properties have been achieved according to API requirements, the process is followed by swelling-parameter testing, which includes the LSM test, accretion test, and erosion test. However, if the mud properties have not been met , the mud samples will be prepared again until the required specifications are achieved. The process is then continued by analyzing the performance and effectiveness of drilling mud containing nanosilica and KCl as shale inhibitors. Finally, the study aims to identify the best mud sample in each swelling-parameter test and determine the potential of nanosilica to replace KCl as a shale inhibitor. The flowchart of this research can be seen in Figure 5.

Determination of mud weight

The determination of mud weight in this study was based on the calculated specific gravity (SG) values for each sample. This laboratory research does not have a designated mud-weight target, which in general is determined through pore pressure–fracture gradient (PPFG) graphs.

Determination of mud properties

In this study, the API standards were used as the standard of mud properties.

Table 3. API specification for drilling mud properties (Darly & Gray 1988)

Mud Properties	API Specification
Viscometer dial reading at 600 rpm (cp)	Min 30
Viscometer dial reading at 300 rpm (cp)	Min 23
Plastic Viscosity (cp)	Min 7
Yield Point (lb/100ft^2)	Max 50
Fluid Loss (ml)	Max 12
pH	9 – 11
YP/PV ratio	Max 3

Table 4. Composition of base fluid (L.D) mud sample

Material	SG	Wt.	Conc.	Vol
	g/ml	g	ppb	ml
Fresh water	1,00		316,78	316,78
pH Controller	2,10		0,50	0,24
Viscosifier 1	2,60		9,00	3,46
LCM	1,50		4,50	3,00
Viscosifier 2	1,50		1,20	0,80
FLCA	1,55		2,25	1,45
Nanosilica	2,40		3,50	1,46
Temperature stabilizer	1,54		4,00	2,60
Bacteria controller	1,02		0,25	0,25
Weighting agent	4,20		90,00	21,43

Table 5. Composition of L.D. + Nanosilica 1% mud sample

Material	SG	Wt. Conc.	Vol
	g/ml	g ppb	ml
Fresh Water	1,00	315,32	315,52
pH Controller	2,10	0,50	0,24
Viscosifier 1	2,60	9,00	3,46
LCM	1,50	4,50	3,00
Viscosifier 2	1,50	1,20	0,80
FLCA	1,55	2,25	1,45
Nanosilica	2,40	3,50	1,46
Temperature Stabilizer	1,54	4,00	2,60
Bacteria Controller	1,02	0,25	0,25
Weighting Agent	4,20	90,00	21,43

Table 6. Composition of L.D. + Nanosilica 3% mud sample

Material	SG	Wt. Conc.	Vol
	g/ml	g ppb	ml
Fresh Water	1,00	312,40	312,40
pH Controller	2,10	0,50	0,24
Viscosifier 1	2,60	9,00	3,46
LCM	1,50	4,50	3,00
Viscosifier 2	1,50	1,20	0,80
FLCA	1,55	2,25	1,45
Nanosilica	2,40	10,50	4,38
Temperature Stabilizer	1,54	4,00	2,60
Bacteria Controller	1,02	0,25	0,25
Weighting Agent	4,20	90,00	21,43

Table 7. Composition of L.D. + KCl 1% mud sample

Material	SG	Wt. Conc.	Vol
	g/ml	g ppb	ml
Fresh Water	1,00	315,01	315,01
pH Controller	2,10	0,50	0,24
Viscosifier 1	2,60	9,00	3,46
LCM	1,50	4,50	3,00
Viscosifier 2	1,50	1,20	0,80
FLCA	1,55	2,25	1,45
KCl	1,98	3,50	1,77
Temperature Stabilizer	1,54	4,00	2,60
Bacteria Controller	1,02	0,25	0,25
Weighting Agent	4,20	90,00	21,43

Table 8. Composition of L.D. + KCl 3% mud sample

Material	SG	Wt. Conc.	Vol
	g/ml	g ppb	ml
Fresh Water	1,00	315,01	315,01
pH Controller	2,10	0,50	0,24
Viscosifier 1	2,60	9,00	3,46
LCM	1,50	4,50	3,00
Viscosifier 2	1,50	1,20	0,80
FLCA	1,55	2,25	1,45
KCl	1,98	10,50	5,30
Temperature Stabilizer	1,54	4,00	2,60
Bacteria Controller	1,02	0,25	0,25
Weighting Agent	4,20	90,00	21,43

Determination and preparation of mud samples

Five mud samples were utilized in this study, consisting of base fluid (L.D.), L.D. + 1% nanosilica, L.D. + 3% nanosilica, L.D. + 1% KCl, and L.D. + 3% KCl. The base fluid serves as a sample that does not contain any shale inhibitor. The variation in nanosilica and KCl concentrations aims to identify the optimal performance and most effective dosage among the samples in addressing shale swelling issues, which will then be compared with mud that lacks any shale inhibitor. The concentrations of nanosilica and KCl were kept the same so that the mud samples could be compared optimally. The concentrations of the other additives were also maintained consistently, except for fresh water, which followed the concentration adjustments of nanosilica and KCl. The detailed compositions of the mud samples are summarized in Tables 4-8.

Density measurement

Mud density measurement using a tool called Pressurized Mud Balance and the material needed is the sample of the mud in after hot rolled condition. The pressurized mud balance is designed differently from a conventional mud balance. In a pressurized mud balance, a plunger is provided that can be used to draw mud from the cup while simultaneously applying pressure to force the mud into the end of the lid. When the plunger can no longer be pressed, it indicates that the cup is filled completely and contains no remaining space for gas or air bubbles, allowing the density measurement to be obtained with higher accuracy.

Rheology measurement

Rheology measurements were performed using a Fann VG Viscometer, a thermo cup, and a thermometer logger to heat and ensure that the mud sample had reached a temperature of 120°F. The mud sample was poured into the thermo cup and left until the thermometer logger indicated that the temperature had reached 120°F. Then take measurements and read the number shown on the dial reading until it is stable at each rpm speed (600, 300, 200, 100, 6 and 3 rpm) and calculate the values of plastic viscosity (PV), yield point (YP), low shear rate yield point (LSRYP), and gel strength (GS).

- $PV = C_{600} - C_{300}$ (1)
- $YP = C_{300} - PV$ (2)
- $LSRYP = (2 \times C_3) - C_6$ (3)

Filtration loss and filter cake measurement

Filtration loss and filter cake measurements were carried out using an API Filter Press. The mud sample was poured into the inner chamber of the cell body up to approximately 60 ml, after which a pressure of about 100 psig was applied while opening the valve. The process was allowed to run for 30 minutes. After 30 minutes, the amount of filtrate produced by the mud sample (ml) was recorded, then the pressure valve was turned off and the pressure was released. The thickness of the filter cake was also measured using a ruler, and the condition of the filter cake was documented.

pH measurement

The pH measurement was performed using a Digital pH Meter. The electrode bracket of the device was cleaned with distilled water, then dried and calibrated using buffer solutions of pH 7, pH 4, and pH 10, ensuring that the electrode bracket remained in a dry condition. After calibration, the pH of the mud was measured by immersing the electrode bracket into the mud sample. The measurement result was recorded, and the reading was allowed time to stabilize on the display.

Potassium (K^+) content measurement

The potassium (K^+) content measurement was carried out using a potassium test kit. This procedure required mud-sample filtrate, sodium perchlorate ($NaClO_4$), and a 10 ml centrifuge tube. A total of 7 ml of mud filtrate was poured into the centrifuge tube at a 90-degree angle, then 3 ml of $NaClO_4$ was added. The tube was then closed and rotated for 1 minute at a speed of 1800 rpm. After centrifugation, the tube was removed, and the volume of the resulting precipitate was read.

Chloride ion content (Cl^-) measurement

The chloride (Cl^-) ion content measurement was performed using several materials, including mud-sample filtrate, phenolphthalein (PP), distilled water, H_2SO_4 (sulfuric acid), potassium chromate, and 0.282 N $AgNO_3$ (silver nitrate 0.01 g). A total of 1 ml of mud filtrate and 3 drops of PP were poured into a beaker, then titrated with 0.01 N H_2SO_4 until the filtrate's initial color appeared. After that, 25 ml of distilled water and 10 drops of potassium chromate were added, and the mixture was titrated with 0.282 N $AgNO_3$ until it turned red or orange.

Methylene blue test (MBT) measurement

The MBT measurement was conducted using several tools and materials. The tools required include an Erlenmeyer flask, a hot stirrer, a stirrer, a magnetic stirrer, a stirring rod, and Whatman paper. The materials needed consist of 2 ml of mud -sample filtrate or cuttings, distilled water, 3% H_2O_2 (hydrogen peroxide), 5N H_2SO_4 (sulfuric acid), 2% tetrasodium pyrophosphate ($Na_4P_2O_7$), and a methylene blue solution with a concentration of 3.2 g/L. The MBT test can be used to determine the bentonite content (using mud-sample filtrate) and to identify the type of clay minerals present (using 1 g of cuttings). All the ingredients used are put into the erlenmeyer flask and heated for 10 minutes at a temperature of 160°C. Condition the sample to the desired temperature, then add distilled water until the total volume reaches 50 mL in the Erlenmeyer flask. Then titrate with methylene blue as much as 0,5 ml or 1 ml until a *halo circle* appears and record the volume of methylene blue used.

Linear swelling meter (LSM) test

The tools used in the LSM test consist of compactors, linear swelling meters, and calipers. The required materials include 20 g of cuttings and a mud sample in after-hot-rolled condition. The cuttings that have been compacted and measured for their thickness are placed into the equipment assembly, after which the mud sample is poured and the software settings are adjusted. The test continues until the graph displayed in the software reaches a plateau condition.

Accretion test

The tools used in the accretion test consist of accretion test containers, monel steel tubes, tweezers, and Silverson mixers. The materials required include a mud sample in after–hot-rolled condition and 20 g of cuttings (14 mesh). The cutting sample was dried at 200°F for 16 hours, then placed into a temperature-neutralized mud sample and mixed using a Silverson mixer for 1 minute at 1000 rpm. Monel steel tubes that has been dried and weighed initially (initial) are then put into the mud sample and stir until the entire surface of the monel is covered by mud sample. Lift and wait for the monel steel tube for 10 seconds, then weigh the weight of the monel. Repeat the test 4 times. Percentage of accretion:

Erosion test

$$\frac{W\ Tube\ After\ Accretion\ -\ W\ Tube\ Initial}{W\ Tube\ Initial} \quad (4)$$

The tools used in the erosion test consist of 14-mesh screens and tweezers. Meanwhile, the materials required include a mud sample, 20 g of cuttings (8 mesh), and salt water. The prepared mud and cutting samples were poured into an aging cell to be hot-rolled for 16 hours at 200°F. After undergoing the hot-rolled process, the cuttings are filtered using a 14-mesh screen and washed thoroughly with salt water until no mud remains on the surface. The cuttings are taken with tweezers and dried in a 220°F oven for 4 hours, then placed in a desiccator for 1 hour. The cuttings are weighed and the results are recorded. They are then re-dried using the oven and desiccator, followed by reweighing and recording the final measurements. Percentage of erosion:

$$\frac{Initial\ Cutting\ Weight\ -\ Remaining\ Cutting\ Weight}{Initial\ Cutting\ Weight} \quad (5)$$

RESULT AND DISCUSSION

Density of mud sample

The first measurement conducted in this study was the determination of mud-sample density. This measurement was performed using a pressurized mud balance, and the results for all mud samples were obtained as follows:

As shown in Table 9. it can be observed that adding 1% and 3% nanosilica or KCl has a similar effect on mud density, namely increasing the density of the mud samples by approximately ±0.1 ppg. However, the increase from 1% to 3% concentrations of nanosilica and KCl did not produce a significant impact on mud density. The change resulted from the addition of nanosilica and KCl was not large enough to be detected by the pressurized mud balance, so the density differences among all samples were not observed as substantial. The accuracy of the pressurized mud balance is stated at 0.1 ppg.

Rheology result

Rheology measurement aims to obtain data on PV, YP, LSRYP, dan gel strength in both conditions, before hot rolled and after hot rolled.

Based on Diagram 1. to Diagram 5. it can be seen that all five mud samples are within the expected rheological target range, as shown in Table 3. However, nanosilica has tends to increase solid particles in the mud because it has a higher PV value compared to the L.D. and KCl samples. Mud samples containing nanosilica also show more stable and higher YP values compared with KCl mud, whose YP decreases significantly by 12 lb/100 ft². The L.D. sample has lower values than both the nanosilica and KCl mud samples. The LSRYP, 10-second GS, and 10-minute GS of the nanosilica samples are found values relatively similar to those of the KCl samples, but demonstrate better performance than the L.D.

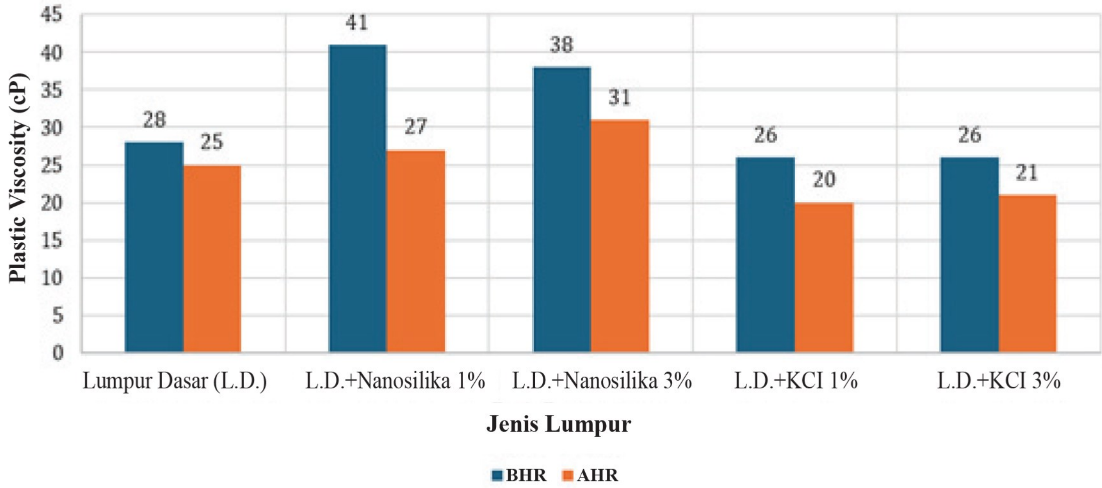

Figure 7. Plastic viscosity comparison

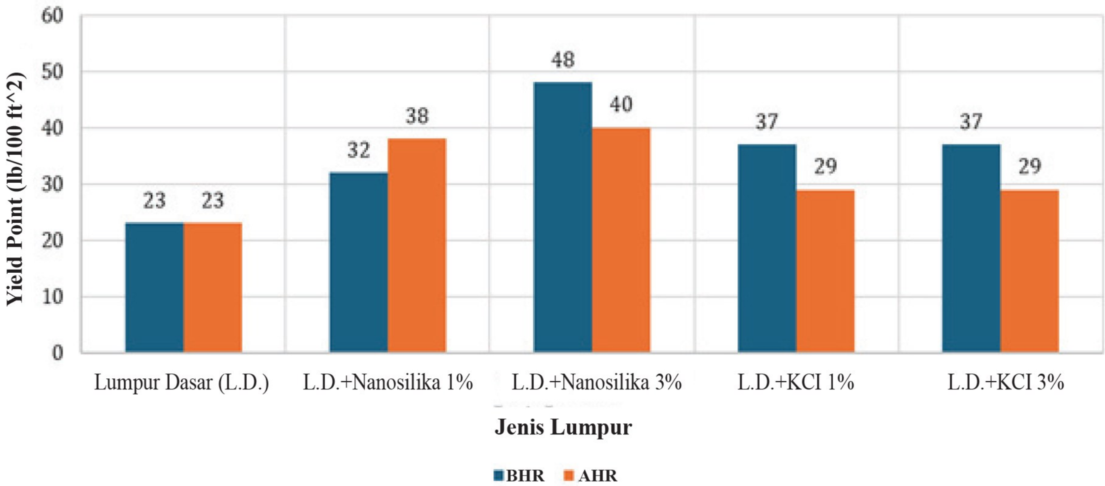

Figure 8. Yield point comparison

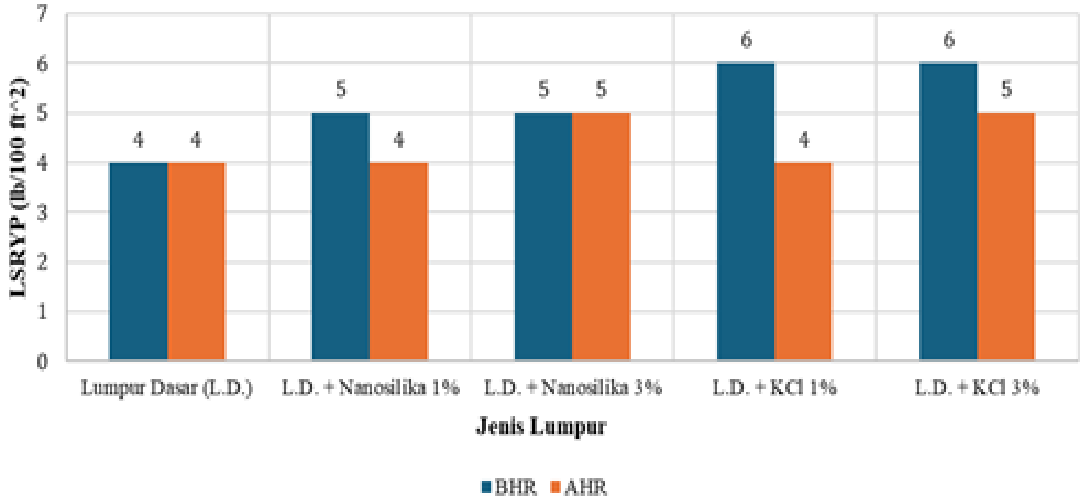

Figure 9. Low shear rate yield point comparison

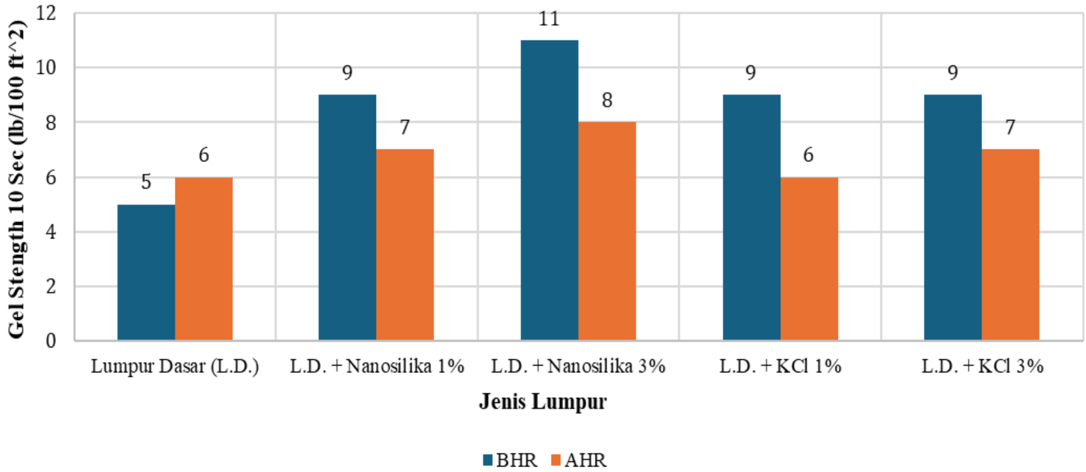

Figure 10. Gel strength 10 sec comparison

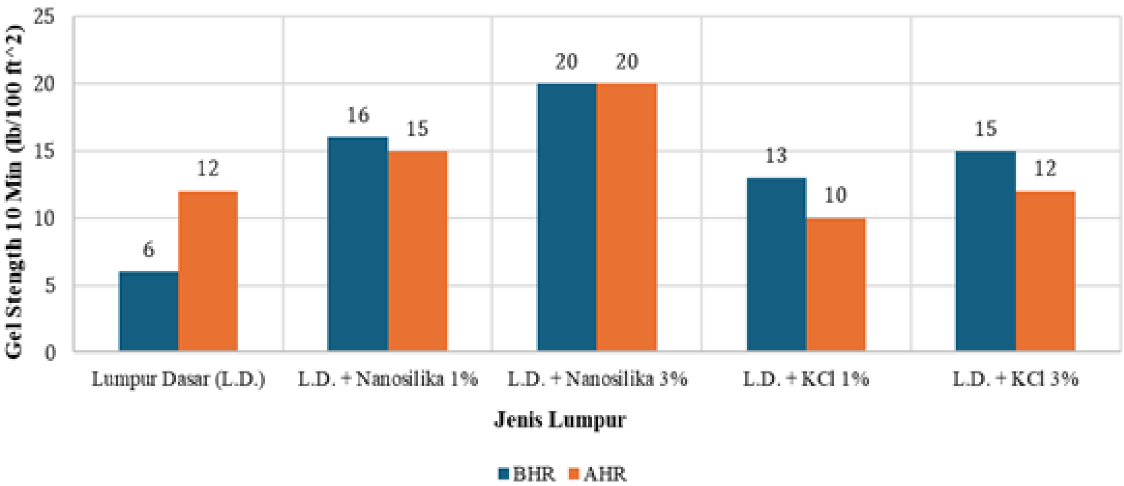

Figure 11. Gel strength 10 min comparison

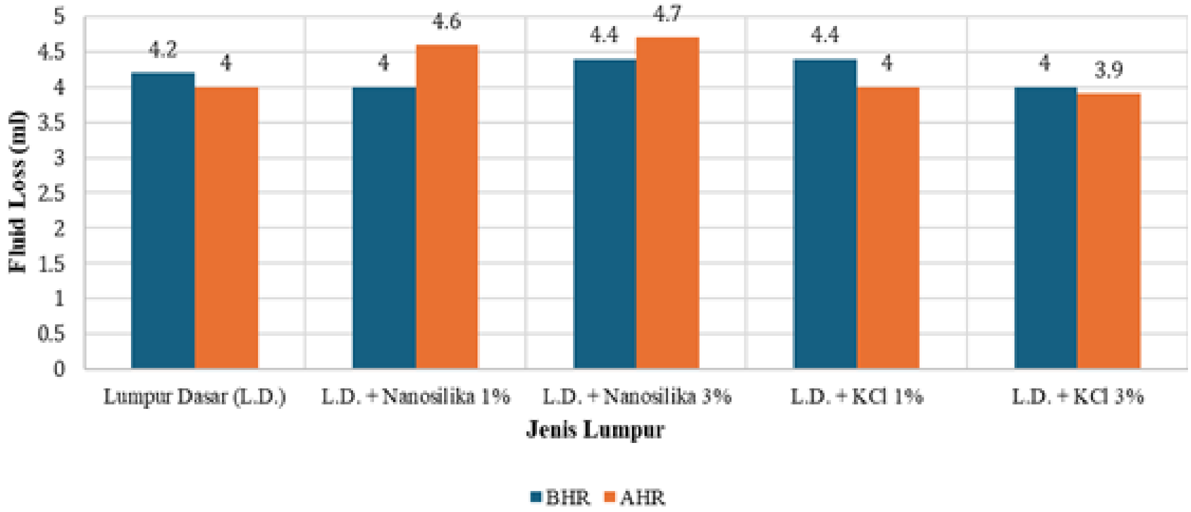

Fig 12. Fluid loss comparison

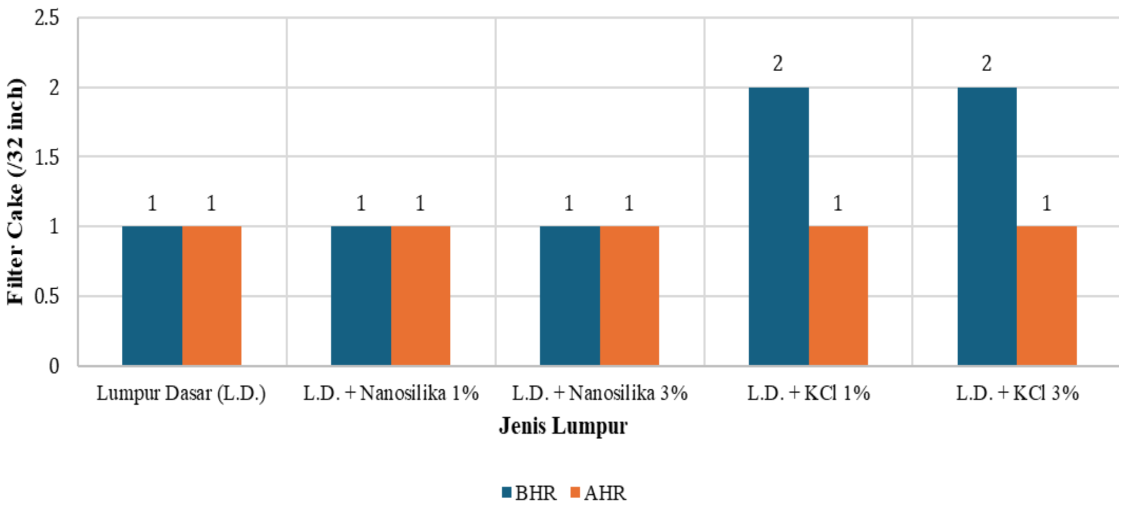

Fig 13. Filter cake comparison

sample. The reduction in rheological properties under AHR conditions may be caused by thermal degradation occurring between particles within the mud (Prakash et al., 2021).

Filtration loss and filter cake

The result of filtration loss and filter cake measurement can be seen below.

Based on Diagram 6. there was observed an increase in fluid loss in the nanosilica samples under AHR conditions, in contrast to the KCl samples, which were shown the ability to reduce the amount of fluid loss produced after hot rolling. According to Hajiabadi et al. (2020), this may occur because higher concentrations of nanosilica tend an increased likelihood of agglomeration between nanosilica particles within the mud. The agglomeration process can lead the formation of larger particle clusters that adhere to one another, creating gaps through which filtrate can pass (Asad et al., 2024). In contrast, within KCl mud, K^+ ions can form aggregates that fill pore spaces, causing the filter cake to become less permeable and thereby reducing fluid loss (Lalji 2022).

Based on Diagram 7. the nanosilica samples were found produced filter cakes with identical thicknesses in both BHR and AHR conditions. In contrast, the KCl samples experienced a reduction in filter-cake thickness under AHR conditions. This shows that nanosilica has the ability to produce filter cake with the same thickness in the BHR and AHR conditions, also does not result in increasing the thickness of the filter cake when compared to L.D. sample.

pH measurement

The measurement of pH value aims to determine the acidity or alkalinity of each mud sample. The pH values for all mud samples can be seen below:

Table 10. pH value of mud samples

Mud Samples	pH Value	
	BHR	AHR
L.D.	11,77	9,94
L.D. + Nanosilica 1%	10,64	9,03
L.D. + Nanosilica 3%	10,11	9,14
L.D. + KCl 1%	10,85	9,76
L.D. + KCl 3%	11,34	9,65

Based on Table 10. all five mud samples were found pH values within the acceptable range for drilling mud. Drilling mud functions effectively at a pH between 9 and 11. This occurs because polymers derived from mud additives are able to work properly only under alkaline conditions. Polymers perform well in such conditions because they are not degraded by acids. This indicates that the polymers in all mud samples can continue to work effectively under both BHR and AHR conditions.

Potassium (K+) content

The measurement of K^+ content aims to determine the concentration of potassium present in mud samples treated with KCl. The K^+ content values for the mud samples are provided in the table below:

Table 11. Potassium content of L.D. sample

		L.D.	
		BHR	AHR
Vol. of Precipitation	mL	-	-
KCl Conc.	Ppb	-	-
K+ Content	mg/L	-	-

Table 12. Potassium content of L.D. + nanosilica 1% sample

		L.D. + Nanosilica 1%	
		BHR	AHR
Vol. of Precipitation	mL	-	-
KCl Conc.	Ppb	-	-
K+ Content	mg/L	-	-

Table 13. Potassium content of L.D. + nanosilica 3% sample

		L.D. + Nanosilica 3%	
		BHR	AHR
Vol. of Precipitation	mL	-	-
KCl Conc.	Ppb	-	-
K+ Content	mg/L	-	-

Table 14. Potassium content of L.D. + KCl 1% sample

		L.D. + KCl 1%	
		BHR	AHR
Vol. of Precipitation	mL	0,10	
KCl Conc.	Ppb	3,17	
K+ Content	mg/L	4751,66	

Table 15. Potassium content of L.D. + KCl 3% sample

		L.D. + KCl 3%	
		BHR	AHR
Vol. of Precipitation	mL	0,60	
KCl Conc.	Ppb	10,99	
K+ Content	mg/L	16491,44	

Based on Table 11. to Table 15. the K^+ content in both KCl samples showed identical results under both BHR and AHR conditions. The increase in K^+ content was clearly influenced by the higher concentration of KCl used in the two samples. The 1% KCl and 3% KCl mud samples displayed good results because both contained KCl concentrations that produced values close to the actual amounts added, namely 3.50 g and 10.00 g. Meanwhile, no K^+ content was detected in the L.D. and nanosilica samples because they did not contain any additives with K^+ ions.

Chloride (Cl-) ion content

The measurement of Cl^- content in the mud samples aims to determine the amount of chloride present, which is used as a reference for the total salt percentage in each mud formulation. The Cl^- content values for the mud samples are provided in the table below:

Table 16. Chloride ion content of L.D. sample

		L.D.	
		BHR	AHR
Vol $AgNO_3$	mL	-	-
Cl^- Content	mg/L	-	-

Table 17. Chloride ion content of L.D. + nanosilica 1% sample

		L.D. + Nanosilica 1%	
		BHR	AHR
Vol $AgNO_3$	mL	-	-
Cl^- Content	mg/L	-	-

Table 18. Chloride ion content of L.D. + nanosilica 3% sample

		L.D. + Nanosilica 3%	
		BHR	AHR
Vol $AgNO_3$	mL	-	-
Cl^- Content	mg/L	-	-

Table 19. Chloride ion content of L.D. + KCl 1%

		L.D. + KCl 1%	
		BHR	AHR
Vol $AgNO_3$	mL	0,74	0,86
Cl^- Content	mg/L	7400,00	8600,00

Table 20. Chloride ion content of L.D. + KCl 3% sample

		L.D. + KCl 3%	
		BHR	AHR
Vol $AgNO_3$	mL	1,92	2,23
Cl^- Content	mg/L	19200,00	22300,00

Based on Table 16. to Table 20. the chloride-ion content in the two KCl mud samples showed noticeable differences, and the increase in Cl^- amount in the 3% KCl sample occurred as a result of the higher KCl concentration used. The osmotic effect in the mud samples is influenced by the chloride content, causing the level of water hydration by the clay to decrease, which in turn reduces the swelling rate. Meanwhile, in the L.D. and nanosilica samples, Cl^- content was not produced because there were no additives containing Cl^- ions.

MBT test

The measurement of MBT value aims to determine the bentonite-equivalent concentration in a mud sample and also can be used to identify the type of clay present in a cutting sample. The MBT values for the mud samples can be seen in the table below:

Table 21. MBT result of L.D. sample

		L.D.	
		BHR	AHR
MBT Vol.	mL	4.00	4.50
MBT for Mud	ppb	10.00	11.25

Table 22. MBT result of L.D. + nanosilica 1% sample

		L.D. + Nanosilica 1%	
		BHR	AHR
MBT Vol.	mL	4.00	4.00
MBT for Mud	ppb	10.00	10.00

Table 23. MBT result of L.D. + nanosilica 3% sample

		L.D. + Nanosilica 3%	
		BHR	**AHR**
MBT Vol.	mL	3.50	5.00
MBT for Mud	ppb	8.75	12.50

Table 24. MBT result of L.D. + KCl 1% sample

		L.D. + KCl 1%	
		BHR	**AHR**
MBT Vol.	mL	3.50	3.00
MBT for Mud	ppb	8.75	7.50

Table 25. MBT result of L.D. + KCl 3% sample

		L.D. + KCl 3%	
		BHR	**AHR**
MBT Vol.	mL	4.00	3.00
MBT for Mud	ppb	10.00	7.50

Based on Table 21. to Table 26. the MBT concentration values in all mud samples were observed fluctuations. A good MBT value is considered a volume that matches or comes close the bentonite concentration used in the mud formulation. This variation may result from the use of an inaccurate mud volume either lower or higher than the required 2 mL.

In addition to being used for determining the bentonite-equivalent content in mud, the MBT test can also be conducted to identify the clay-mineral content in a cutting sample. In this study, the MBT test was also performed to determine the type of clay minerals present in the cuttings used for the LSM, accretion, and erosion tests. After the cutting samples were tested, the MBT volume was found reached 29 ml, corresponding to a CEC value of 29 Meq/100 g. According to Table 1. the clay contained in the cutting sample is montmorillonite & illite.

Linear swelling meter test

LSM testing aims to determine the level of swelling caused by the fluid used. In this study, the LSM test was carried out for 117 hours, and the testing was stopped once the graph showed a plateau. Based on the LSM test conducted using cuttings, the following results were obtained.

Table 26. Potential swelling profile (cutting)

Fluid Name	**Swelling (%)**
L.D.	21,8%
L.D. + Nanosilica 1%	15,3%
L.D. + Nanosilica 3%	16,8%
L.D. + KCl 1%	12,2%
L.D. + KCl 3%	13,6%
Aquadest	18,5%

Based on Table 27. it can be observed that mud containing KCl demonstrates better performance compared with mud formulated with nanosilica and the base fluid, as indicated by its lower swelling percentages (12.2% and 13.6%). The L.D. + The 1% KCl sample had a lower swelling percentage than the L.D. + 3% KCl sample, indicating that 1% KCl represented the optimal usage limit in this study. The potential for flocculation at a 3% KCl concentration can lead a higher swelling percentage in the L.D. + 3% KCl sample. Increasing the ionic concentration of KCl can cause flocculation (McClements, 2004). The strong ionic interactions of KCl can also create an imbalance in other additives particularly polymers thereby reducing the effectiveness of polymer performance.

The L.D. + nanosilica 1% sample also had a smaller swelling percentage than the L.D. + nanosilica 3% sample due to the agglomeration of nanosilica particles, which prevented the fluid from optimally entering the clay pores and caused an increase in swelling percentage. The swelling percentages produced by the nanosilica sample and the KCl sample did not differ significantly, which indicates the potential of nanosilica as a shale inhibitor, even though it is not performing as optimally as KCl. In addition, both the nanosilica and KCl samples show lower swelling percentages compared with the L.D. sample. The sample demonstrating the best performance in the LSM test was found been the L.D. + 1% KCl mud sample.

Accretion test

The accretion test aims to identify which mud sample has the best ability to avoid sticking metal

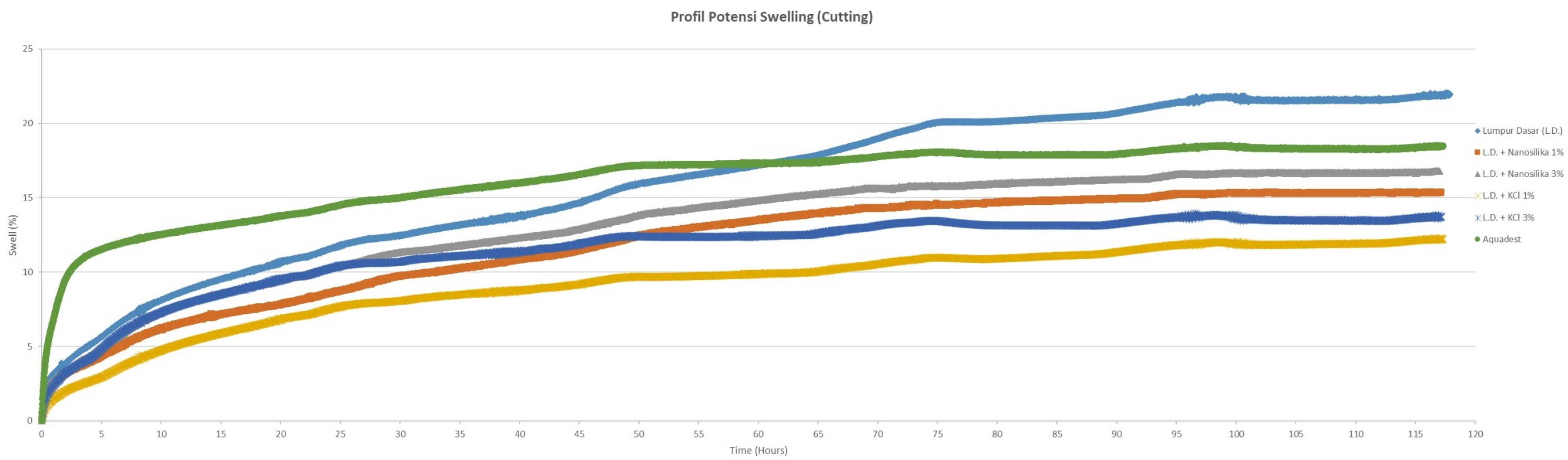

Figure 14. Potential swelling profile (cutting)

surfaces. The results of the accretion test are provided as follows:

Table 27. Accretion data of L.D. sample

Fluid Name	W Tube Initial (g)	W Tube After Accretion (g)
L.D.	114,68 130,15	15,47
	114,68 129,39	14,71
	114,68 129,85	15,17
	114,68 128,66	13,98
	%Accretion	14,8325 14,83

Table 28. Accretion data of L.D. + nanosilica 1% sample

Fluid Name	W Tube Initial (g)	W Tube After Accretion (g)
L.D. + Nanosilica 1%	114,68 132,9	18,22
	114,68 130,15	15,47
	114,68 131,11	16,43
	114,68 131,67	16,99
	%Accretion	16,7775 16,78

Table 29. Accretion data of L.D. + nanosilica 3% sample

Fluid Name	W Tube Initial (g)	W Tube After Accretion (g)
L.D. + Nanosilica 3%	114,68 138,68	24
	114,68 135,24	20,56
	114,68 133,19	18,51
	114,68 133,74	19,06
	%Accretion	20,5325 20,53

Based on Table 27. to Table 31. it can be seen that L.D. + KCl 3% is the best sample in this test, characterized by the lowest accretion percentage value among other mud samples. The higher the concentration of inhibitors used, the lower level of hydration of water to clay which results in a decrease in the sticky properties of clay (Cliffe & Young, 2008). While the L.D. + nanosilica 3% sample is the worst sample, this can occur due to the agglomeration of nanosilica particles resulting in nanosilica particles to sticking to each other and sticking to the surface of the monel (adhesion force). In contrat to KCl, nanosilica has a hydroxyl group (-OH) that reacts with water and causes nanosilica to insoluble in water, which results in agglomeration between nanosilica particles. Nanosilica mud were not optimal in this test because they had a higher accretion percentage than the L.D. sample, indicating the high ability of nanosilica to stick to the drillstring, resulting in bit balling and stuck pipe.

Table 30. Accretion data of L.D. + KCl 1% sample

Fluid Name	W Tube Initial (g)	W Tube After Accretion (g)
L.D. + KCl 1%	114,68 126,5	11,82
	114,68 126,56	11,88
	114,68 125,87	11,19
	114,68 126,49	11,81
	%Accretion	11,675 11,68

Table 31. Accretion data of L.D. + KCl 3% sample

Fluid Name	W Tube Initial (g)	W Tube After Accretion (g)
L.D. + KCl 3%	114,68 127,68	13
	114,68 125,93	11,25
	114,68 125,47	10,79
	114,68 125,42	10,74
	%Accretion	11,445 11,45

Erosion test

The erosion test aims to find out the best type of mud prevent erosion in cutting. The erosion test was carried out once with two weighing repetitions. The result of the erosion test are attached to the table as follows:

Table 32. Erosion test data (1st Weighing)

Fluid Name	Initial W (g)	Remaining W (g)	%Erosion Test
L.D.	20,06	6,25	68,84%
L.D. + Nanosilica 1%	20,08	14,04	30,08%
L.D. + Nanosilica 3%	20,15	11,84	41,24%
L.D. + KCl 1%	20,05	14,61	27,13%
L.D. + KCl 3%	20,02	13,68	31,67%

Table 33. Erosion test data (2nd Weighing)

Fluid Name	Initial W (g)	Remaining W (g)	%Erosion Test
L.D.	20,06	6,25	68,84%
L.D. + Nanosilica 1%	20,08	14,04	30,08%
L.D. + Nanosilica 3%	20,15	11,84	41,24%
L.D. + KCl 1%	20,05	14,61	27,13%
L.D. + KCl 3%	20,02	13,68	31,67%

Based on Table 32. and Table 33. the average value in the L.D. sample was 68,965%, L.D. + nanosilica 1% was 29,93%, L.D. + nanosilica 3% was 41,115%, L.D. + KCl 1% was 27,055%, and L.D. + KCl 3% was 31,695%. Based on the average value of the five samples, it can be seen that sample with the best performance in the erosion test is L.D. + KCl 1%. Both 3% nanosilica and 3% KCl produce a higher erosion percentage than the 1% concentration. This can occur due to the excessive ionic interaction so that it actually results in excessive flocculation that is not compact, cutting will be easier to disperse because of its not strong (compact) and cohesive structure. In addition, the agglomeration of nanosilica will cause clumping and accumulation that creates weak points and can be eroded if it has reached the weakest point. Besides, nanosilica samples have the potential to replace KCl because they have a lower erosion percentage than L.D. sample and the resulting erosion percentage range is not too far between 1% nanosilica and 1% KCl (±2,8% – 2,95%).

Increased hydrogen bonding between nanoparticles may cause particle agglomeration at higher concentrations of nanosilica 3%. Higher accretion values indicate that this type of agglomeration can form larger clusters that increase adhesion to metal surfaces and reduce the efficiency of pore plugging. Because irregular aggregates may create micro-channels that allow fluid migration, this also helps to explain the higher filtration loss observed at 3% nanosilica. On the other hand, KCl primarily prevents swelling through ionic exchange: within the clay interlayer, K^+ replaces Na^+, which reduces osmotic swelling pressure. The balance between providing sufficient ionic strength to inhibit hydration and the destabilizing effect of high electrolyte concentrations on polymer additives is reflected in the greater effectiveness of 1% KCl compared with 3%.

Based on all tests of mud physical properties and swelling parameters that have been conducted, the samples containing nanosilica show the potential to replace KCl as a shale inhibitor, supported by the dual working mechanisms—physical and chemical—that nanosilica is understood. Although the accretion test showed a relatively low effectiveness of nanosilica as a shale inhibitor, the results produced in the LSM and erosion tests indicated the potential of nanosilica to function in this role, reinforced by the physical-property measurements of the mud that had been conducted earlier. From this study, it can be concluded that the mud sample demonstrating the best overall performance based on swelling-parameter testing was the L.D. + 1% KCl sample, as indicated by its lowest swelling and erosion percentages compared with the other four samples.

CONCLUSION

Based on the swelling-parameter tests, the mud sample showing the best performance in the linear swelling meter test was the L.D. + 1% KCl formulation, while the best result in the accretion test was obtained from the L.D. + 3% KCl sample. In the erosion test, the L.D. + 1% KCl sample performed the best overall result. These findings suggest that nanosilica has not been able fully replace the function of KCl as a shale inhibitor, yet it can compete because its performance does not differ greatly from that of mud samples containing KCl.

Based on the swelling-parameter tests, particularly the LSM results, the performance of KCl remains superior to that of nanosilica, even though nanosilica operates through two mechanisms—physical and chemical. This indicates that the cation-exchange mechanism of KCl is functioning more effectively than the working mechanisms of nanosilica.

The L.D. + 1% KCl sample excels in the erosion test, while the L.D. + 3% KCl sample performs best in the accretion test. KCl remains more effective than nanosilica because nanosilica particles tend to agglomerate, which causes them to clump together and increase the likelihood of erosion.

Nanosilica samples produce rheological values—particularly PV, YP, and GS—that are shown higher measurements compared with KCl mud. The values generated by the nanosilica samples remain within the acceptable range and tend to perform better than those of the KCl samples. Nanosilica is found to be less optimal in controlling filtrate because there was observed an increase in filtrate volume under AHR conditions. This may occur due to agglomeration between nanosilica particles and interactions between nanosilica and other mud additives. Even so, nanosilica is able to produce filter cakes with more stable thickness and maintain good physical structure.

Based on the pH values, both the nanosilica and KCl mud samples demonstrate good performance, as indicated by their pH values falling within the alkaline range of 9–11. Both types of mud are able to function effectively because the polymers in the formulations can work optimally under alkaline conditions, where they are not degraded by acids. Based on the LSM test, the accretion test, and the erosion test, nanosilica has not been able fully replace the role of KCl as a shale inhibitor, although it shows promising potential even if its performance is not achieving the same level of effectiveness as KCl. Furthermore, nanosilica demonstrates a strong advantage in improving the rheological properties of drilling mud.

ACKNOWLEDGEMENT

The authors grateful to PT. Pertamina Technology Development I (TD1) and Geosains Laboratory Pertamina Research & Technology Innovation (RTI) for its cooperation and support. Moreover, the authors are also would like to thank UPN "Veteran" Yogyakarta, and all stakeholders who have assisted in the preparation of this journal.

GLOSSARY OF TERMS

Unit	Definition	Symbol
AHR	After Hot Rolled	
BHR	Before Hot Rolled	
CEC	Cation Exchange Capacity	Meq/100gr
Cl^-	Chloride	
FLCA	Fluid Loss Control Agent	
g	Gram	
GS	Gel Strength	lb/100ft^2
H_2O_2	Hydrogen Peroxide	
H_2SO_4	Sulfuric Acid	
KCl	Potassium Chloride	
K^+	Potassium	
LCM	Loss Circulation Material	
L.D.	Lumpur Dasar (Base Fluid)	
LSM	Linear Swelling Meter	
LSRYP	Low Shear Rate Yield Point	lb/100ft^2
MBT	Methylene Blue Test	mL
$NaClO_4$	Sodium Perchlorate	
$Na_4P_2O_7$	Tetrasodium Phyrosphate	
PP	Phenolphthalien	
PV (μ_∞)	Plastic Viscosity	cP
SG	Specific Gravity	
W	Weight	Grams
WBM	Water Based Mud	
YP	Yield Point	lb/100ft^2
ρ	Fluid Density	
γ	Shear Rate	
τ	Shear Stress	
μ	Viscosity	
τ_o	Yield Stress	

REFERENCES

Asad, M. S., Jaafar, M. T., Rashid, F. L., Togun, H., Rasheed, M. K., Al-Obaidi, M. A., ... & Sarris, I. E. (2024). Sustainable Drilling Fluids: A Review of Nano-Additives for Improved Performance and Reduced Environmental Impact. Processes, 12(10), 2180.

Basic Petroleum Geology and Log Analysis. (2001). Halliburton.

Cliffe, S., & Young, S. (2008). Agglomeration and accretion of drill cuttings in water-based fluids. In AADE-08-DF-HO-10 AADE Fluids Conference and Exhibition held.

Darly, H.C.H. and Gray, G.R. 1988. Composition and Properties of Drilling and Completion, published by Gulf publishing Company, Houston

Gbadamosi, A. O., Junin, R., Oseh, J. O., Agi, A., Yekeen, N., Abdalla, Y., ... & Yusuff, A. S. (2018, August). Improving hole cleaning efficiency using nanosilica in water-based drilling mud. In SPE Nigeria annual international conference and exhibition (pp. SPE-193401). SPE.

Guo, W., Guo, X., Chang, M., & Dai, W. (2018). Evaluating the effect of hydrophobic nanosilica on the viscoelasticity property of asphalt and asphalt mixture. Materials, 11(11), 2328.

Hajiabadi, S. H., Bedrikovetsky, P., Mahani, H., Khoshsima, A., Aghaei, H., Kalateh-Aghamohammadi, M., & Habibi, S. (2020). Effects of surface modified nanosilica on drilling fluid and formation damage. Journal of Petroleum Science and Engineering, 194, 107559.

Hughes, B. (2006). Drilling fluids reference manual. Houston, Texas.

Jakubiak, S., Tomaszewska, J., Jackiewicz, A., Michalski, J., & Kurzyd³owski, K. J. (2016). Polypropylene–zinc oxide nanorod hybrid material for applications in separation processes. Chemical and Process Engineering, 37(3).

Kartini, R. (2014). Lumpur berbasis air rendah padatan dan tahan temperatur tinggi bagi pemboran di formasi shale. Lembaran Publikasi Minyak dan Gas Bumi (LPMGB), 48(2), 111–118.https://doi.org/10.29017/LPMGB.48.2.1217

Kumari, N., & Mohan, C. (2021). Basics of clay minerals and their characteristic properties. Clay Clay Miner, 24(1), 1-29.

Kwaw, J. A. (2018). Effect Of Salinity (KCl) on ROP and Rheological Properties Concerning Water Base Mud Formulations. Politecnico Di Torino Department of Environment, Land and Infrastructuren Engineering.

Lalji, S. M., Ali, S. I., Haneef, J., Quraishi, R., Kapadia, A., & Jawaid, H. (2022). Changes in Pakistan crude oil properties contaminated by water-based drilling fluids with varying KCL concentrations. Chemical Papers, 76(7), 4189-4201.

McClements, D. J. (2004). Protein-stabilized emulsions. Current opinion in colloid & interface science, 9(5), 305-313.

Mondshine, T. C., & Kercheville, J. D. (1966). Successful gumbo-shale drilling. Oil and Gas Journal, 64(13), 194.

Mujiyanti, D. R., Nuryono, N., & Kunarti, E. S. (2010). Sintesis dan karakterisasi silika gel dari abu sekam padi yang diimobilisasi dengan 3-(trimetoksisilil)-1-propantiol. Jurnal Berkala Ilmiah Sains dan Terapan Kimia, 4(2), 150-167.

Nabhani, N., & Emami, M. (2012). The potential impact of nanomaterials in oil drilling industry. Nano con, 201, 23-25.

Nirmala, G. S., Natsir, R., & Zikra, M. (2025). The recovery factor analysis on heavy oil under electromagnetic heating treatment. Scientific Contributions Oil & Gas, 48(2), 1–9. https://doi.org/10.29017/scog.v48i2.173

Prakash, V., Sharma, N., & Bhattacharya, M. (2021). Effect of silica nano particles on the rheological and HTHP filtration properties of environment friendly additive in water-based drilling fluid. Journal of Petroleum Exploration and Production Technology, 11, 4253-4267.

Prastiyanto, A., Azmiyawati, C., & Darmawan, A. (2008). Pengaruh penambahan merkaptobenzotiazol (MBT) terhadap kemampuan adsorpsi gel silika dari kaca pada ion logam Kadmium.

Saleh, T. A., Rana, A., Arfaj, M. K., & Ibrahim, M. A. (2022). Hydrophobic polymer-modified nanosilica as effective shale inhibitor for water-based drilling mud. Journal of Petroleum Science and Engineering, 209, 109868.

Swaco, M. (1998). Drilling Fluids Engineering Manual. MI Swaco.

Taraghikhah, S., Mohammadi, M. K., & Nowtaraki, K. T. (2017, October). Now It is the Time to Forget Potassium Based Shale Inhibitors by Developing Nano Silica-Alumina Based Drilling Fluid; Laboratory Study Proves Improvement in Shale Inhibition and Temperature Stability. In SPE Asia Pacific Oil and Gas Conference and Exhibition (p. D012S036R076). SPE.

Trivana, L., Sugiarti, S., & Rohaeti, E. (2015). Sintesis dan karakterisasi natrium silikat (Na2SiO3) dari sekam padi. Jurnal Sains & Teknologi Lingkungan, 7(2), 66-75.

Wahyudi, P., & Makmur, T. (2004). Test of formation water and chemical compatibility. Scientific Contributions Oil & Gas (LEMIGAS), 27(3), 12–17. https://doi.org/10.29017/SCOG.27.3.1054

Wahyuni, V. S., Fathan, M. R., & Ulfah, B. M. (2025). Uji laboratorium: Analisis berat lumpur pemboran pada sumur can. JUTIN: Jurnal Teknik Industri Terintegrasi, 8(4), 4048–4054. https://doi.org/10.31004/jutin.v8i4.5022

Zhang, L., & Li, H. (2024). Nanosilica applications in water-based mud. In G. Zhuang & P. Yuan (Eds.), Clay science in drilling and drilling fluids (Vol. 11, pp. 45–72). Elsevier. https://doi.org/10.1016/B978-0-443-15598-7.00001-.